

# Lab on a Chip

Accepted Manuscript



This is an *Accepted Manuscript*, which has been through the Royal Society of Chemistry peer review process and has been accepted for publication.

*Accepted Manuscripts* are published online shortly after acceptance, before technical editing, formatting and proof reading. Using this free service, authors can make their results available to the community, in citable form, before we publish the edited article. We will replace this *Accepted Manuscript* with the edited and formatted *Advance Article* as soon as it is available.

You can find more information about *Accepted Manuscripts* in the [Information for Authors](#).

Please note that technical editing may introduce minor changes to the text and/or graphics, which may alter content. The journal's standard [Terms & Conditions](#) and the [Ethical guidelines](#) still apply. In no event shall the Royal Society of Chemistry be held responsible for any errors or omissions in this *Accepted Manuscript* or any consequences arising from the use of any information it contains.

# Title:

---

FISH in Chips: Turning microfluidic Fluorescent In Situ Hybridization into a quantitative and clinically reliable molecular diagnosis tool.

# Authors and affiliations:

---

**Karla Perez-Toralla<sup>a,b,c</sup>, Guillaume Mottet<sup>a</sup>, Ezgi Tulukcuoglu Guneri<sup>a</sup>, Jérôme Champ<sup>a</sup>, François-Clément Bidard<sup>d</sup>, Jean-Yves Pierga<sup>d,e</sup>, Jerzy Klijanienko<sup>f</sup>, Irena Draskovic<sup>g</sup>, Laurent Malaquin<sup>a</sup>, Jean-Louis Viovy<sup>a</sup>, Stéphanie Descroix<sup>a</sup>**

<sup>a</sup> *Macromolecules and Microsystems in Biology and Medicine, Institut Curie, Centre National de Recherche Scientifique, Université Pierre et Marie Curie, UMR 168, 75005 Paris, France*

<sup>b</sup> *Univ Paris Diderot, Sorbonne Paris Cité, F-75205, Paris, France*

<sup>c</sup> *current address: Université Paris Sorbonne Cité; INSERM UMR-S1147; Centre Universitaire des Saints-Pères, 45 rue des Saints-Pères, 75270 Paris Cedex 06, France*

<sup>d</sup> *Department of Medical Oncology, Institut Curie, 26 rue d'Ulm, 75005 Paris, France.*

<sup>e</sup> *Université Paris Descartes, Paris, France*

<sup>f</sup> *Department of Pathology, Institut Curie*

<sup>g</sup> *Telomeres & Cancer laboratory, Institut Curie, UPMC Univ. Paris 06, Equipe Labellisé « Ligue », Paris, France*

# Abstract:

---

Microfluidic systems bears promise to provide new powerful tools for the molecular characterization of cancer cells, in particular for the routine detection of multiple cancer biomarkers using a minute amount of sample. However, taking miniaturized cell-based assays into the clinics requires the implementation and validation of complex biological protocols on chip, as well as the development of disposable microdevices produced at low cost. Based on a recently developed microfluidic chip made of Cyclo Olefin Copolymer for cell immobilization with minimal dead volume and controlled shear stress, we developed a protocol performed entirely in liquid phase, allowing the immobilization and fixation of cells, and their quantitative characterization by fluorescence in situ hybridization. We demonstrated first on cell lines, and then on two clinical case studies, the potential of this method to perform quantitative copy number measurement and clinical scoring of the amplification of the *ERBB2* gene, a decisive biomarker for the prescription of HER2+ related targeted therapies. This validation was performed in a blind protocol on two clinical case studies, in reference with the gold standard and clinically used method based on glass slides. We obtained a comparable reproducibility, and a minor difference in apparent amplification, which can be corrected by internal calibration. The method thus reaches the standards of robustness needed for clinical use. The protocol can be fully automated, and its consumption of sample and DNA probes is reduced as compared to glass slides protocols by factors at least 10. Total duration of the assay is divided by two.

37

38

## 39 Introduction

---

40

41 With the development of personalized medicine and targeted therapies in oncology, cancer patient  
42 management is now driven by the molecular alterations, mainly somatic mutations, detected in the  
43 tumor cells. A paradigmatic case is the *ERBB2* gene (v-erb-b2 erythroblastic leukemia viral oncogene  
44 homolog 2), located in chromosome 17. This proto-oncogene, involved in the regulation of cell  
45 growth and proliferation, is amplified in about 15% of breast cancers. This amplification leads to the  
46 overexpression of the corresponding protein on cell membrane named HER2<sup>1</sup>. Breast cancers  
47 harbouring *ERBB2* amplification are usually of high tumor grade and were historically associated with  
48 a poor prognosis. In the early 2000's, trastuzumab, a monoclonal antibody directed against the  
49 extracellular part of HER2, demonstrated a very high anti-tumor efficacy. Other anti-HER2 therapies  
50 have been developed for this subgroup of breast cancers, whereas trastuzumab was also shown to be  
51 effective in other *ERBB2*-amplified tumors, such as in a subgroup of metastatic gastric cancers. HER2  
52 status assessment is currently part of the daily routine management of breast and gastric cancers.

53 The assessment of HER2 status on tumor tissue is strictly codified by the American Society of Clinical  
54 Oncology and the College of American Pathologists (ASCO/CAP) guidelines<sup>2</sup>. Membranous HER2  
55 protein over-expression can be assessed by immunohistostaining (IHC) or In-situ Hybridization (using  
56 fluorescent (FISH) or chromogenic (CISH) probes). IHC is semi-quantitative at best, and since HER2 is  
57 also expressed in non-amplified cells to a weaker extent, it yields ambiguous cases, with a suboptimal  
58 inter-reader reproducibility. Moreover, this technique is considered as not reliable for cytological  
59 samples. In situ hybridization is in contrast a quantitative detection method that allows determining  
60 the exact number of copies of the *ERBB2* gene per chromosome 17 on a cell-by-cell basis  
61 (*ERBB2*/SE17 ratio)<sup>3</sup>. Indeed, to distinguish an increase in the number of chromosomes (polysomy)  
62 from a real *ERBB2* amplification, targeting the centromeric region of chromosome 17 (SE17) used as  
63 an internal control is crucial.

64 Thus, to provide a valid assessment of the HER2 status of cytological samples, FISH is used as the  
65 “gold standard”. However, the use of FISH in routine clinical practice has remained limited, in spite of  
66 its recognized superiority and inter-reader reproducibility over IHC. This is largely due to its high cost  
67 and technically demanding character, despite the use of robots for the numerous sequential  
68 incubations of glass slides required in conventional protocols.

69 Implementing FISH analysis on microfluidic platforms has gained a lot of interest, since it offers the  
70 possibility to create more compact and low cost automated platforms, while reducing the  
71 consumption of sample and reagents, in particular DNA probes. Being able to perform all the steps of  
72 the FISH protocol, from sample preparation to detection, in a closed chip can also help to reduce the  
73 risk of contamination or loss of precious samples. However, building an integrated and quantitative  
74 device for FISH analysis of real samples remains challenging: first, as for most cell-based assays,  
75 sample preparation on chip must be performed with caution, in order to immobilize cells on the  
76 surface with a high cell density, while avoiding cell overlapping. Shear stress should also be reduced  
77 during this step to limit the risk of cell disruption inside the confined channels. Second, the design  
78 and fabrication of the microfluidic platform should be optimized to allow the delivery of precise  
79 volumes of complex mixtures and reagents with different viscosities into the reaction chamber in a  
80 serial manner, without inducing cross contamination; precise temperature control is also an  
81 important parameter during the different steps of the FISH protocol. Finally, the chip should be  
82 compatible with high magnification fluorescence imaging for efficient FISH signal detection and  
83 quantification.

84 Taking in consideration all these technical requirements, up to now only few examples of proof-of-  
85 concept miniaturized FISH platforms have been proposed in the literature<sup>4-8</sup>. Their primary focus has  
86 mostly been technological, showing different strategies to reduce the cost of the test by reducing the  
87 volume of all FISH reagents, in particular DNA probes (the most expensive reagent) required per  
88 sample (by 10 to 30-fold) as well as the labor time (by 10-fold). The pioneer work of Sieben et al.<sup>4</sup> was  
89 based on the integration of elastomeric valves, pumps and thin-film platinum heaters inside narrow

90 microchannels (chemically etched in glass substrates) with low dead volume, in order to build a fully  
91 automated FISH platform. In this work, however, the fabrication process involved complex  
92 technologies and required the use of a clean room environment increasing the cost of the test (100 \$  
93 per chip). Using an integrated heating system can be an advantage for local and precise temperature  
94 control but it also requires important technical skills for a proper calibration prior to each use. A  
95 similar automated platform has been proposed more recently<sup>7</sup>, employing a suction-type pump to  
96 deliver samples and reagents to a dedicated reaction chamber, while controlling their temperature  
97 using an external thermoelectric cooling module. These improvements decreased to some extent the  
98 sophistication level of the device and thus the fabrication cost (based on soft-lithography  
99 techniques), but the multilayer process required during the assembly of the micropump remains  
100 time-consuming. Another strategy aiming at improving the robustness of the cell immobilization step  
101 on the chip surface, has been developed using a simpler device made with PDMS microchannels  
102 reversibly bonded to nanoengineered glass slides<sup>5</sup>. This architecture was very efficient in enhancing  
103 the adhesion and confinement of cell suspensions, thus offering the possibility to enrich samples with  
104 low cellular content. However, the procedure could not be fully automatized since it required manual  
105 handling and removal of the PDMS lid to complete the FISH protocol following the conventional  
106 procedures for glass slides, thus reducing automation potential, and increasing the risk of sample  
107 contamination. Moreover, this approach requires expensive and complex fabrication procedures  
108 involving glass slides with TiO<sub>2</sub> assembled nanoclusters. Finally, a recent study has proposed to  
109 implement micropatterning based methods to create a functionalized array of “cell-adhesive” islands  
110 on glass slides and enable the precise positioning of single cells to expedite the image acquisition  
111 step<sup>8</sup>. Although, this work demonstrates the possibility to perform large-scale high-throughput FISH  
112 analysis, no modification of the standard FISH protocol was performed and the cell patterning  
113 process remains laborious.

114 These examples demonstrate the benefit of microfluidic devices for cellular assays, but they mostly  
115 ignore another important aspect in the transition of microfluidic protocols to the clinical world, i.e.

116 chip cost. Indeed, it is no use reducing reagents consumption, if this gain is lost in the additional cost  
117 of the chip production, operation or storage, as compared to a glass slide (the standard support for  
118 FISH analysis). PDMS, for instance is very popular for fast prototyping, but it presents many inherent  
119 drawbacks<sup>9</sup> (e.g. high water and gas permeability, swellability by most organic solvents, notably  
120 alcohols). These features make its use inconvenient for FISH assays, which require the use of solvents  
121 and thermal treatments. The production of PDMS chips is also rather expensive. In contrast,  
122 thermoplastic materials such as Cyclic Olefin Polymers (COP) and Cyclic Olefin Copolymers (COC)  
123 present many assets for future routine clinical use<sup>10-13</sup>. They are available at very low cost (typically in  
124 the order of a few \$ per kg for bulk raw material), in different grades resistant to harsh solvents and  
125 temperatures up to 180°C. They also present excellent optical quality in the visible and UV ranges,  
126 allowing for high quality fluorescence imaging and they exist in grades approved for clinical use. Last  
127 but not least, they are amenable to high resolution and high throughput microforming by hot  
128 embossing or injection molding for routine mass-production of monolithic and fully disposable  
129 devices. The small scale production of COC chips with custom designs still require an initial  
130 investment<sup>14,15</sup>, but routine production can drop costs dramatically, typically to a few \$ per chip or  
131 less.

132 Thus, in our aim to develop a device transposable to routine clinical use, we selected COC as the  
133 fabrication material, and a design previously conceived by our group to solve some of the problems  
134 mentioned above<sup>16</sup>. This device combines a simple design, small footprint and allows the  
135 implementation of standard biological protocols in a chip format with low volume consumption. The  
136 chip design was optimized from a hydrodynamic point of view to provide a flexible and efficient  
137 platform for the immobilization and analysis of cells. This new design also allowed us to obtain a high  
138 density monolayer of intact and non-overlapping cells, which is crucial for cell based assay. This  
139 feature was achieved thanks to the laminarity of the flow and to the absence of stagnation areas in  
140 the chamber, the latter arising from its 3 dimensional “slanted” walls. We also demonstrated the

141 possibility to perform FISH imaging. However, this earlier version did not have the automation or the  
142 quantification power needed for clinical scoring applications.

143 Thus, so far none of the previously described microfluidic FISH platforms and protocols, including  
144 ours, has been pushed to a level of robustness and quantitiveness suitable for clinical applications.

145 They involved proof-of-concept experiments with a direct transposition of the standard FISH protocol,  
146 providing “yes or no” results with no quantitative analysis of gene amplification and scoring, as  
147 needed e.g. for the assessment of *ERBB2* amplification.

148 In the present work, we try to bridge this gap, and build upon our earlier successful proof of  
149 concept<sup>16</sup>, to develop a complete, simple on-chip FISH protocol suitable for quantitative molecular  
150 typing in a clinical setting, while keeping low production and operation costs. As an application, we  
151 selected the quantitative assessment of the number of copies of the *ERBB2* gene, and of a reference  
152 in the centromeric region measuring polysomy of chromosome 17. As recalled in the literature, this  
153 typing is currently of paramount importance in treatment orientation for breast cancer patients:  
154 originally, the *ERBB2* gene amplification has been associated with aggressive tumors and a negative,  
155 more pessimistic prognostic for patients treated with conventional methods. Targeted therapies for  
156 these types of tumors have been developed, however, and have considerably improved the outcome  
157 and prognostic for these patients. Thus, we believe that this application constitutes both a route to a  
158 rapid and extremely useful new application of microfluidic technologies in real life, and a challenge to  
159 promote the maturation of lab on chip technologies, and demonstrate their potential in applications  
160 as demanding as clinical diagnosis.

161 We first quantified the HER2 status of two different cancer cell lines through high resolution  
162 microscopy, and compared the results with those of a conventional protocol on glass slides  
163 considered as the current gold standard. We also evaluated the scoring provided by our method  
164 regarding two samples from breast cancer patients.

165



# 166 Experimental Section

---

## 167 1. Materials

168 Cyclic olefin copolymer (COC) films (Topas® 8007,  $T_g = 80^\circ\text{C}$ , 145  $\mu\text{m}$  thick) and plates (Topas® 8007,  $T_g$   
169 =  $80^\circ\text{C}$ , 5 mm thick) were purchased from Topas Advanced Polymers, Extrusion Lab (Germany). 2-  
170 Hydroxyethyl cellulose –HEC – (average  $M_v \sim 90,000$ ), Poly-L-lysine –PLL – solution (mol wt 150,000-  
171 300,000, 0.01%, sterile-filtered) and pepsin lyophilized powder (from porcine gastric mucosa; 3,200-  
172 4,500 units/mg protein) were purchased from Sigma-Aldrich (USA). The ready-to-use FISH probes (ON  
173 ERBB2, HER2/*neu* (17q12) / SE17), the FISH Hybridization Buffer (FHB), DAPI (4',6-diamidino-2-  
174 phenylindole) counterstain (1 $\mu\text{g}/\text{mL}$ ) and counterstain diluents were purchased from Kreatech  
175 Diagnostics (The Netherlands). SuperFrost® Plus glass slides were purchased from Menzel-Gläser  
176 (Germany). Cell culture reagents were purchased from Gibco, Life Technologies (USA).

## 177 2. Microfluidic device design and fabrication

178 The details and hydrodynamic characterization of the chip are described elsewhere<sup>16</sup>. In brief, the  
179 chip design (Figure 1 a) consists in a dual structure comprising narrow channels (height=30  $\mu\text{m}$ ,  
180 width=60  $\mu\text{m}$ ) and large 3D chambers (height=0.38 mm, bottom diameter=1 mm). The device was  
181 prepared in COC plates using a hot embossing procedure as described<sup>16,17</sup>. A solvent assisted  
182 plasticizing process<sup>18</sup> was used to bond a thin COC film to the embossed microfluidic plate (25mm  $\times$   
183 35mm and 5 mm thick), thus providing a monolithic, fully disposable chip. The COC film has a  
184 thickness (145  $\mu\text{m}$ ) comparable with that of glass coverslips, in order to allow high resolution imaging  
185 with objectives up to 100X oil immersion.

186 In our previous work, fluid handling was performed manually<sup>16</sup>. Here, to increase reproducibility and  
187 prepare for a clinical environment, this chip was associated with a fully programmable pressure-  
188 based fluid handling platform. Tygon (Cole-Parmer) and Polytetrafluoroethylene (PTFE) tubes (inner  
189 diameter: 0.028 mm) were used for the fluidic connections. The COC chip was coupled with a flow

190 control system (MFCS, Fluigent) for the injection of all reagents. A double layer coating was used for  
191 the surface treatment of the COC microchannels to render the surface hydrophilic and avoid non-  
192 specific adsorption of proteins<sup>19</sup>, and at the same time to enable the attachment of the cells to the  
193 bottom surface of the 3D chambers<sup>20</sup> (Figure 1 b). The procedure was the following: first, 200  $\mu$ L of  
194 HEC solution (2 % wt in Phosphate-Buffered Saline -PBS- 1X) were injected in the channels and let to  
195 incubate (1h at room temperature -RT-). After a rinsing step with PBS, the microchannels were filled  
196 with 100  $\mu$ L of PLL, let to incubate (3 hours at 37°C) and washed with PBS prior to the injection of  
197 cells.

198 The thermal control of the chip was provided by a high precision hot plate (Stuart Equipment, UK)  
199 coupled with a temperature probe (Implementable Thermocouple probe, Thermo Fisher Scientific)  
200 that was inserted in the chip.

### 201 **3. Cell culture:**

202 The human epithelial cell lines SKBR-3 (*ERBB2* amplified breast adenocarcinoma) and G-401 (*ERBB2*  
203 unamplified rhabdoid tumor) were obtained from the American Type Culture collection (Manassas,  
204 VA). Cells were cultured in Dulbecco's modified Eagle's medium (high glucose) supplemented with  
205 10% heat-inactivated fetal bovine serum, 100 units/mL aqueous penicillin, 100  $\mu$ g/mL streptomycin  
206 and 2 mM L-glutamine, at 37°C in a humidified atmosphere with 5% of carbon dioxide.

### 207 **4. Sample preparation:**

208 For cell lines, the confluent culture cells were detached by a trypsin treatment (0.05% Trypsin-EDTA  
209 1X), centrifuged and re-suspended in 1mL culture medium to obtain an approximate concentration of  
210  $10^6$  cells/mL. For the standard FISH protocol, five glass slides were placed at the bottom of a Petri dish  
211 (10 cm in diameter) filled with 25 mL of culture medium. 180  $\mu$ L of cell suspension were added on top  
212 of each glass slide by manual pipetting, covering the entire surface of the glass slide. The cells were

213 then allowed to adhere properly and spread on the glass slides, overnight (37°C with 5% CO<sub>2</sub>). The  
214 culture medium was finally removed, and the slides were washed with PBS 1X buffer two times.  
215 The remaining cell suspension (100 µL) was kept at room temperature for at most 5 minutes, and the  
216 desired volume was injected in the COC chip for the miniaturized FISH experiments. The procedure  
217 for cell immobilization on chip has been previously described<sup>16</sup>. It is based on the use of a PLL surface  
218 treatment to enable cell adhesion on the COC surface. This was combined with a novel 3D chip design  
219 which creates strong flow velocity contrasts between the deep chambers and the low profile  
220 connection channels. This allows confining cells over a restricted area (with low flow velocity)  
221 whereas no cells remain in the connecting channels (Figure 1 a). The design also allows a minimal  
222 dead volume on the chip thanks to the small size of the connecting channels and of the chambers  
223 (total volume of 2 µL), avoidance of stagnation points in the flow, and optimal fluid replacement with  
224 a minimal rinsing volume. The workflow follows three different steps: first, cell injection, then an  
225 incubation step (5 minutes with no flow rate) during which cells are allowed to adhere to the surface;  
226 finally a washing step with PBS 1X buffer to remove non adhered cells.

227 Pleural effusions: two different samples were obtained from pleural effusions from two *ERBB2*-  
228 amplified metastatic breast cancer patients. These patients presented with dyspnea due to metastatic  
229 pleural effusion and had pleural punctures as part of their usual clinical management. Following  
230 patients consent, pleural effusions were transferred to the laboratory instead of being discarded.  
231 Samples were analyzed in parallel in a blind protocol, by a combination of cytology (May-Grünwald-  
232 Giemsa stain) and FISH performed on glass slides on the one hand (at the department of Pathology,  
233 Institut Curie), and by FISH using the COC chip on the other hand, without prior knowledge of the  
234 nature of the cell content in the samples. Prior to the FISH on-chip analysis, red blood cells,  
235 polynuclear cells and plasma were removed using a Ficoll density gradient, and the mono-nucleated  
236 cells were obtained in 100 mL of sample. This enriched sample was re-suspended in PBS 1X to reach a  
237 total volume of 500 µL and 15 µL of the cell suspension were injected in the chip for FISH analysis.

## 238 **5. Fluorescence in situ hybridization (FISH) protocol**

239 The efficiency and sensitivity of the FISH protocol were first validated using cells immobilized on glass  
240 slides. This conventional protocol was used as a reference in terms of signal quality, copy number  
241 enumeration and preservation of cell morphology during the implementation of the FISH protocol on  
242 chip. Glass slide experiments were performed in parallel for each FISH experiment on chip as a  
243 control.

244 Slides were first incubated in SSC 2X buffer (diluted from SSC 20X, pH~7) at 37°C for 2 minutes. The  
245 samples were pre-treated with pepsin (0.05 µg/mL in 0.01 M HCl) for 7 minutes at 37°C, washed in  
246 one change of PBS 1X and one change of SSC 2X at room temperature. The slides were then fixed  
247 with Carnoy's Fixative (Acetic acid/ethanol 1:3 (v/v)) at 5°C during 20 minutes and then rinsed with  
248 SSC 2X two times (10 minutes at 37°C and 2 minutes at room temperature). The cells were then  
249 dehydrated by ethanol (respectively with 70%, 90% and 100%, 2 minutes for each solution) and dried  
250 at room temperature. The hybridization mix (10 µL of labelled DNA probes) was applied on the slides  
251 and covered with a glass coverslip. DNA probes were co-denatured at 75°C for 15 min and then  
252 incubated at 37°C overnight in a humid atmosphere. Unbounded/non-specifically bounded probes  
253 were removed by standard procedures : first in washing solution I (0,4X SSC +0.3% NP40, pH~7) for 3  
254 minutes at 72°C and then in washing solution II (2X SSC +0.1% NP40, pH~7) for 3 minutes at room  
255 temperature. Finally, following the dehydration step, 10 µL of DAPI (diluted at a concentration of 0.2  
256 µg/mL in counterstain diluent) was applied on the cells and covered with a glass coverslip.

257 For the implementation of the FISH protocol on chip, we miniaturized the standard procedure (Table  
258 1) and performed several modifications of the standard protocol to gain a better compatibility with  
259 our system (See Results and discussion section for rationale). New alternatives were developed (Table  
260 1, steps 7 and 12) to implement the FISH protocol in a flow through format, taking inspiration from<sup>21</sup>.  
261 The short washing steps involved in glass slides protocols were also replaced by a continuous flow  
262 washing step on chip to increase efficiency. The concentration of pepsin solution for the enzymatic  
263 digestion step (Table 1, step 3) was increased from 0.05 µg/mL to 1 µg/mL. Finally, the 10 µL of FISH

264 probes were replaced by 2.5  $\mu$ L of probe diluted in 2.5  $\mu$ L of FHB, contributing to a strong reduction  
265 of reagents costs. The duration and temperature of the different incubation steps were kept constant.  
266 For the analysis of cells from the pleural effusions on chip, a supplementary step of RNase treatment  
267 (0.1mg/mL, at 37°C for 1 hour) was added after the fixation step. It was followed by two rinsing steps,  
268 first at room temperature with 100  $\mu$ L SSC 2X (200mbars) and then at 37°C for 10 minutes in SSC 2X.

## 269 **6. Image acquisition and treatment**

270 Imaging of the labelled cells on glass slides and on chip was performed using an epi-fluorescence  
271 microscope (Nikon Eclipse 80i) equipped with a piezo focus lens positioner (P-721 PIFOC<sup>®</sup>, Germany),  
272 a high speed CCD camera (CoolSNAP HQ2, Photometrics, Roper scientific - Princeton instruments), a  
273 mercury lamp (HGFIL Lampe 130 W) and adequate filter sets (DAPI, GFP, RHOD). The images were  
274 taken using an oil immersion 100X objective (Nikon, CFI Plan Apo VC, NA 1.4, WD 0.13). Fluorescence  
275 images for each set of filters were recorded using the MetaMorph<sup>®</sup> Imaging Software (Molecular  
276 Devices). The step of the piezo scanner was set at 0.2  $\mu$ m in order to acquire high resolution 3D  
277 images (z stacks, 5-20  $\mu$ m scan total length) (Figure 1 b). Before image analysis, the “Meinel”  
278 algorithm for 3D deconvolution of fluorescence signals was applied to the recorded z stacks<sup>22</sup>.

## 279 **7. FISH probes and HER2 scoring criteria**

280 According to 2013 the ASCO/CAP guidelines<sup>2</sup>, gene amplification using dual-probe assays is defined as  
281 a *ERBB2*/*SE17* ratio  $\geq$  2.0 with an average *ERBB2* copy number  $\geq$  4.0 signals. In the presence of  
282 chromosomal abnormalities, like aneusomy of chromosome 17 (polysomy and monosomy), samples  
283 with a *ERBB2*/*SE17* ratio  $<$  2.0 will be considered as amplified only if they present an average *ERBB2*  
284 copy number  $\geq$  6.0 signals. If the average *ERBB2* copy number is  $<$  4.0 signals the sample will be  
285 negative. Other rare or equivocal cases are explained in detail on the ASCO/CAP guidelines<sup>2</sup>. Thus,  
286 both *ERBB2* and *SE17* copy numbers must be quantified in each cell. The *ERBB2* specific probe is  
287 labelled with a red dye (PlatinumBright 550) and the control DNA probe for the centromere of

288 chromosome 17 (SE17) is labelled with a green dye (PlatinumBright 495). For the FISH experiments  
289 on chip, the FISH probe was diluted at the desired concentration using FHB.  
290 FISH analysis was performed by fluorescence microscopy as described above. Only single, non-  
291 overlapping and intact nuclei were scored. For each nucleus, red and green signals were counted  
292 separately using the ImageJ software (<http://rsb.info.nih.gov/ij>). The *ERBB2* amplification score was  
293 calculated as the ratio of the total *ERBB2* signals to the total SE17 signals counted on a single cell  
294 basis, over at least 20 different cells for each experiment.  
295

## 296 Results and Discussion

---

### 297 1. Technological transfer of FISH protocol from glass slide to COC chip

298 Implementing a cellular assay in a microfluidic format often requires redesigning the protocol of the  
299 bioassay. Among cellular assays, FISH is considered as a complex and demanding process. It consists  
300 of at least seven steps involving the use of organic solvents, dehydration and drying, heating  
301 combined with enzymatic digestion as well as DNA hybridization. A direct transposition of the FISH  
302 protocol performed on glass slides did not yield reproducible and accurate enough results, and a  
303 major reconsideration of the protocol was necessary.

304 The development and optimization of the on-chip protocol were performed with cell lines and using a  
305 FISH probe targeting the centromeric region of chromosome 17. The diploid G-401 cell line was used  
306 as a control. According to the supplier recommendations, an efficient FISH protocol should result in  
307 round, smoothly defined and correctly stained nuclei giving bright, compact and discrete  
308 fluorescence signals. The absence of non-specific hybridization signals or background fluorescence is  
309 also an important criterion for successful signal enumeration. For FISH experiments with the G-401  
310 cell lines, two bright spots should be present inside each nucleus. Split signals in very close proximity,  
311 typical of cells having passed through the S phase of the cell cycle, were counted as one signal.

#### 312 1.1. Flow-through “all wet” FISH protocol on chip

313 Several parameters were modified to optimize the standard FISH protocol with regards to the specific  
314 requirements of miniaturization. A major concern in miniaturized assays is the increased importance  
315 of surface properties, a consequence of the higher surface to volume ratio. As an illustration, a 20-  
316 fold increase in the enzyme concentration was necessary to circumvent the non-specific adsorption  
317 of these molecules to the COC surface, and efficiently digest the proteins of the immobilized cells.  
318 The duration of each step in the protocol was also modified as compared to the glass slide protocol,  
319 to take into account the different kinetics induced by miniaturization and by the continuous flow-

320 through nature of the incubation. Temperature, flow rate and buffer composition were also optimized  
321 (data not shown). Here we only present in more detail a protocol modification that was crucial for the  
322 implementation of a flow-through protocol in closed COC microchannels.

323 In a standard FISH protocol on glass slides, cells are dehydrated by a series of ethanol solutions (e.g.  
324 70%, 90% and 100%) and dried (Table 1). Dehydration by ethanol is expected to promote DNA  
325 condensation and promote its firm adhesion to the surface. It is also expected to help to eliminate  
326 any traces of buffer or reagent (e.g. fixative solution) that may inactivate the probes. After that,  
327 however, ethanol must be thoroughly removed, since it may hamper hybridization and proper  
328 diffusion of the FISH probes through the nucleus. From a practical point of view, on glass slides it is  
329 also simpler to seal the probe under a cover slip with rubber cement when the slide is dry.

330 Indeed, most of earlier on-chip protocols retained a drying step. This has been achieved by opening  
331 the chip during part of the protocol<sup>5,6,8</sup> and returning to an “open air” protocol close to that used on  
332 glass slides. We wanted to avoid this approach, which strongly reduces the potential of microfluidics  
333 for full automation. Sieben et al.<sup>4</sup> performed the whole protocol in a closed channel, but flushed air in  
334 the chip. In our hands and in our COC chip, this approach did not yield reproducible enough results,  
335 and we identified several possible reasons for that: at these small scales, wetting phenomena are  
336 critical, and it is difficult to prevent residual fluids to remain in the chip, especially in corners, when  
337 air is pushed through. This can yield poor rinsing, crystal deposition, and even clogging problems.  
338 Also, controlling the dehydration and drying steps inside COC chips remains challenging and prone to  
339 artefacts. As most thermoplastics, COC is not permeable to gas, and the drying process through  
340 ethanol evaporation in closed channels is very slow (up to a few hours at room temperature). The  
341 consequence of a partial drying can be dramatic, since the presence of ethanol in the channels results  
342 in the aggregation and degradation of the DNA probes, decreasing the FISH efficiency (Figure 2 a).  
343 PDMS could be better than COC in this respect, since it adsorbs ethanol quite extensively, but then  
344 the ethanol may be slowly released in the chip during the remainder of the protocol, in a poorly



345 controlled manner, and affect the efficiency and reproducibility of hybridization. Besides, as discussed  
346 in the introduction, we wanted to avoid PDMS, which is not a good candidate for routine clinical use.  
347 To overcome the above problems, we proposed a new FISH protocol where ethanol dehydration steps  
348 are replaced by a washing step with SSC 2X buffer at room temperature. We evaluated the  
349 performance of this new protocol performing microfluidic FISH on G401 cell lines and comparing it to  
350 the standard FISH protocol on glass slides. The results showed that we obtained a robust and  
351 reproducible FISH protocol in the COC chip (counted signals per cell  $\pm$  S.D.:  $1.98 \pm 0.15$ ). This result is  
352 comparable with the control on glass slides (Figure 2 b) (counted signals per cell  $\pm$  S.D.:  $2 \pm 0$ ). We did  
353 not observe any cell with more than two SE17 signals, showing that the hybridization was specific and  
354 that the post-hybridization washing step was efficient to remove non-specifically bounded probes.  
355 This is an important result since we were able to successfully adapt the FISH protocol to our system  
356 by modifying a critical step, without decreasing the efficiency of the hybridization or inducing any  
357 change in the morphology of nuclei.

### 358 **1.2. Reducing the amount of FISH probe and the cost per test**

359 Once the on-chip protocol has been established, we took advantage of miniaturization to decrease  
360 the final cost of the FISH analysis. The use of microfluidics has provided a drastic reduction of the  
361 volume of all reagents (SSC 2X buffer, protease and fixatives solutions, washing solutions I and II,  
362 counterstaining and mounting medium) from the milliliter to the microliter scale (Table 1). This not  
363 only reduces further the cost of the test but it also facilitates the handling of fluids and eliminates  
364 some fastidious steps of the FISH protocol.

365 We also investigated the possibility to decrease the required amount of probe. Indeed, fluorescently  
366 labelled DNA probes are the most expensive reagent of the FISH assay (10  $\mu$ L of probe at 1x are  
367 needed for one experiment on glass slide), as compared to the other reagents. With the design  
368 proposed in this work, the volume of probe needed to perform one test was reduced to 2  $\mu$ L (5 fold  
369 reduction). In order to reach submicroliter amounts of probes, previous works have proposed to

370 decrease the inner volume of the chip<sup>4,5</sup>. However, this requires to drastically reducing the  
371 dimensions of the channels, thus generating higher shear stress that may severely damage cells.  
372 Therefore, we propose here an alternative strategy, taking advantage of the faster and better  
373 controlled kinetics achieved in flow-through miniaturized chips, to further decrease the amount of  
374 probe required, while keeping shear stress to a harmless level. We investigated the efficiency of serial  
375 dilutions of the probe as compared to the concentration usually used on glass slides ( $[C]=1x$ ). Three  
376 different concentrations of probe were investigated on chip ( $[C]=1x$ ,  $[C]=0.5x$  and  $[C]=0.25x$ ). To  
377 characterize the efficiency of probe hybridization for each concentration in the FISH protocol on chip,  
378 we evaluated the signal-to-noise ratio (SNR) of the SE17 signals and compared it with the SNR of  
379 signals from cells analyzed on glass slides. SNR measurements comparing the fluorescence intensity  
380 from the FISH signals and the background fluorescence in the area of the nucleus outside the FISH  
381 signals can be used as an objective method to compare the quality of fluorescence signals in FISH  
382 analysis, and to measure the intensity variability of the FISH signals from cell-to-cell and from two  
383 different sets of experimental conditions<sup>23</sup>.

384 Regardless of the probe concentration, all the scored cells contained two clearly distinguishable and  
385 bright SE17 signals (Figure 3 b, c and d), showing no loss of signals as compared to the standard  
386 concentration of probe on glass slide (Figure 3 e). The signal-to-noise ratio was also equivalent for all  
387 the different probe concentrations on chip (Figure 3 a), as compared to the control glass slides  
388 ( $[C]=1x$ ), showing that the hybridization efficiency was well preserved. Interestingly, similar reduction  
389 of probe concentration in the conventional glass slide protocol (which is not recommended by kit  
390 providers) yielded an increase in the number of the poorly labelled and non-analysable cells (data not  
391 shown). The possibility to use, without such damage lower probe concentration in our chip protocol *a*  
392 *posteriori* justifies our assumption, that the laminar flow pattern in our microfluidic system yields a  
393 better efficiency and reproducibility of probe transport and renewal, and thus better hybridization at  
394 lower probe concentration. This high efficiency could also be a consequence of the absence of a  
395 drying step in our protocol: drying induces a collapse of all macromolecular structures, including

396 DNA, into a compact highly entangled state, promoting the formation of irreversible bonds or micro-  
397 aggregates. Thus, upon re-swelling with the hybridization solution, genomic DNA probably does not  
398 recover the same availability and permeability as before drying. It is then plausible that both  
399 efficiency and kinetics of hybridization could be lower than with a “fully wet” protocol.

400 Considering that the volume of the chip is 2  $\mu$ L, the three different concentrations that have been  
401 tested correspond to a reduction in the amount of probe needed for one sample by 5, 10 and 20-fold,  
402 respectively, with no significant modification of the signal-to-noise ratio as compared to the “gold  
403 standard”. As compared to previous works dealing with the miniaturization of FISH protocols on  
404 chip<sup>4,5</sup> this is an important step towards a significant reduction in the cost of the assay while  
405 preserving its quality.

## 406 **2. HER2 scoring by FISH: COC chips vs. glass slides**

407 In order to take miniaturized cell bioassays into the clinics and take over conventional analysis tools, it  
408 is important to go beyond proof-of-concept FISH experiments on chip<sup>4-8</sup> that show only qualitative  
409 gene identification and check the potential of our microfluidic platform and optimized protocol for  
410 quantitative scoring.

### 411 **2.1. Validating the FISH assay using cell lines**

412 Diagnosis requires to clearly distinguishing a polysomy of chromosome 17, on which trastuzumab  
413 based treatments bring no advantage, from a real *ERBB2* gene amplification, defined as the presence  
414 of multiple copies of the gene per chromosome 17. In order to evaluate the potential of our method  
415 in this respect, we first used two cell lines representing different situations. The G-401 diploid cell line  
416 is used as an “unamplified” control, without polysomy of chromosome 17. These cells must present  
417 two red and two green dots (*ERBB2/SE17* ratio equal to 1). The SKBR-3 cell line was used as a model  
418 for gene amplification (*ERBB2/SE17* ratio greater than 2). SKBR-3 is a hypertriploid human cell line  
419 with a modal chromosome number of 84, occurring in 34% of cells (American Type Culture Collection

420 website). Consistent with previous reports<sup>24</sup>, we measured for these cells an average of 7 copies of  
421 chromosome 17 and more than 30 copies of the *ERBB2* gene per cell.

422 Representative fluorescence images of the FISH analysis for HER2 scoring are depicted in Figure 4.  
423 They were performed for both cell lines immobilized on glass slides and on the COC chip. The flow-  
424 through FISH protocol provided bright and homogeneous SE17 and *ERBB2* spots on chip for both cell  
425 lines. The signal to noise ratio was comparable to the results on glass slides (Figure 4). FISH results on  
426 chip showed a low fluorescence background and no non-specific signals outside the nuclei, which are  
427 important requirements for reliable signal enumeration and HER2 scoring. The high image quality  
428 also shows the excellent optical properties of the COC material (no optical distortions and no  
429 autofluorescence) and the efficiency of the double-layer surface treatment. One also observes a good  
430 preservation of the nuclei morphology inside the COC chip, as compared to the glass slides, showing  
431 that the shear stress in the 3D chambers was maintained at harmless levels, and no cells were  
432 damaged or deformed during the experiment.

433 This new protocol involves a significant gain in the overall protocol duration: in the COC chip, cells can  
434 be immobilized and attached to the bottom surface of the 3D chambers in less than 15 minutes<sup>16</sup>,  
435 without the need of thermal treatments or harsh fixatives that can over cross-link cell proteins and  
436 decrease FISH efficiency<sup>8</sup>. The conventional protocols on glass slides require an incubation of cells  
437 overnight to ensure cell attachment. The counterpart for this gain was a slight increase in the  
438 thickness of cells. The preservation of the three-dimensional shape of nuclei on chip, as compared to  
439 glass slides where the cells are present in a more “flat” configuration, has also been observed in  
440 other microfluidic platforms using other cell immobilization protocols<sup>23</sup>. This can be very useful  
441 during morphological cell analyses, but for the FISH application contemplated here, it requires to  
442 optimize the fluorescence imaging process and the image post-processing (Figure 1 b), in order to  
443 circumvent the possibility of FISH signals overlapping on the z axis. This is particularly critical for  
444 epithelial cancer cells, which can present important shape variations, and be much larger (diameter  
445 of around 40–42  $\mu\text{m}$ ) than e.g. normal or blood cells (diameter of 8–11  $\mu\text{m}$ )<sup>25</sup>, and for cells with high

446 gene amplification levels such as SKBR-3 cells, but also cells from HER2 positive patients. These  
447 requirements have not been mentioned during the development of previous FISH platforms, using  
448 different DNA probes and targets, where only 2 to 4 signals needed to be analysed per cell<sup>4,5</sup>, but  
449 they are crucial for efficient HER2 scoring. In our analysis, we thus used 3D deconvolution microscopy  
450 and analysed a stack of focal planes along the z axis. As compared to glass slides, the additional  
451 scanning time is compensated by the compactness and good distribution of the cells in the chip,  
452 which reduces the area to be scanned.

453 On a quantitative ground, the results for HER2 scoring on chip are presented in Figure 5, showing the  
454 average scores obtained using the G-401 and SKBR-3 cell lines. The error bars show the standard  
455 deviation from the scores obtained from n cells. We obtained a reproducibility of the FISH protocol  
456 on chip comparable with that of glass slides for both cell lines. For the G-401 cell line, the average  
457 *ERBB2/SE17* ratio on chip corresponds to the expected value ( $ERBB2/SE17 = 0.99 \pm 0.07$ ) and stands  
458 well below the *ERBB2* amplification threshold, in good agreement with the “unamplified” status of  
459 this cell line. For the SKBR-3 cell line, the average *ERBB2/SE17* ratio for experiments on chip  
460 ( $ERBB2/SE17 = 3.7 \pm 1.3$ ) was somewhat lower than the results obtained using conventional glass  
461 slides ( $ERBB2/SE17 = 4.62 \pm 1.1$ ). However scores for both methods were well above the *ERBB2*  
462 amplification threshold given by the ASCO/CAP guidelines recommendation (*ERBB2/SE17* ratio  $\geq 2.0$   
463 with an average *ERBB2* copy number  $\geq 4.0$  signals) in good agreement with the “amplified” status of  
464 this cell line (Figure 5). The important cell-cell variability for the SKBR-3 cells, could be explained by  
465 the important genetic dispersion of this cell line<sup>24,26</sup>.

466 Thus, as a summary, the reproducibility and reliability of scoring in the new on-chip FISH protocol is  
467 comparable with that of the conventional one on glass slides, but the measured amplification is in  
468 average slightly lower in the new protocol. As mentioned above, our SSC “all aqueous” treatment  
469 involves a faster and more “gentle” treatment of the cell’s DNA, since there is no dehydration, and  
470 the incubation is much shorter. It was indeed noticed that cells inside the COC chip did present a  
471 more “round” configuration, as compared to cells adhered to the glass slide in the conventional

472 protocol. This may induce some differences in the availability of the target sequences, and thus a  
473 slight difference in measured amplification.

474 Also, although FISH on glass slides is currently considered the “gold standard”, it may itself be prone  
475 to some bias. For instance, it may artificially over-evaluate the number of copies, as a consequence of  
476 the more “harsh” effect of the protocol (involving condensation, drying and re-swelling of nuclear  
477 DNA), which could split some positive chromosomal regions, and this artefact may depend on the  
478 target gene length and location. In any case, we insist, on the fact that this difference is consistent  
479 and reproducible, and the dispersion on data for the chip results is comparable with that obtained on  
480 glass slides and reminiscent of the previously reported standard deviation of this cell line<sup>24</sup>. Thus, it  
481 can be corrected by a suitable cross calibration, and will not affect the quality and significance of  
482 scoring.

483 We acknowledge that an equivalent error bar size, combined with a slightly lower apparent  
484 amplification, may increase the number of ambiguous cases. However, first the discrepancy is small,  
485 so the impact will be low. Second, the current amplification threshold of 2 is itself an empirical value,  
486 with a clinical rather than biological basis, and established with the conventional FISH method that is  
487 itself not absolute. Thus, we are confident that a well-conducted clinical validation of our protocol  
488 will be able to provide a correction to the threshold, which will restore a number of ambiguous cases  
489 not higher than that obtained with the current protocols. Finally, one may recall that the ASCO/CAP  
490 guidelines have already taken into account the possibility of ambiguous scoring and provided  
491 independent criteria to help clinicians in such situations<sup>2</sup>.

## 492 **2.2. Validating the FISH assay on chip using patient samples**

493 After the above quantitative validation of the method with cell lines presenting (in average) a stable  
494 and known amplification score, we also demonstrated the possibility to perform our FISH on-chip  
495 protocol on real samples with different cellular contents in a complex matrix. As a proof of concept,  
496 we tested pleural effusions from two breast cancer patients. This liquid sample typically contains

497 mesothelial cells from the pleura mixed with tumor cells, platelets, red and white blood cells,  
498 proteins, and lipids. In some cases it can also show signs of infection, e.g. bacteria. As pleural effusion  
499 can be considered as a material representative of metastasis and given its complexity, it appears to be  
500 an interesting sample to evaluate the clinical performances of our microfluidic platform. It is  
501 important to notice that the primary tumor from both patients had been previously analysed by  
502 immunohistochemistry, and classified as HER2-positive.

503 We were able to immobilize several subpopulations of cells from the pleural effusion with different  
504 morphologies and sizes of nucleus (from 6 to 10  $\mu\text{m}$  in diameter in the first sample and up to 20  $\mu\text{m}$   
505 in second sample) showing that the COC device is compatible with the use of real and complex  
506 clinical samples (Figure S1 in Supplementary Information and Figure 6 a). For the first patient sample  
507 (sample A), the analysis by FISH in our device did not show any *ERBB2* amplification, indicating that  
508 the immobilized cells were merely leukocytes or mesothelial cells (Figure S1). The cytological  
509 evaluation of the fluid performed in parallel did not show any evidence of malignant cells or  
510 infectious material. Therefore, no further FISH analysis was performed on glass slide by the  
511 pathologist.

512 For the second sample (sample B), we observed different populations of cells with clear and distinct  
513 *ERBB2* and SE17 signals, and no signs of cell deformation: some small cells (probably lymphocytes)  
514 presented no polysomy of the chromosome 17 and no *ERBB2* amplification ( $ERBB2/SE17 = 1$ ); some  
515 big cells with *ERBB2* amplification but without polysomy, and some bigger cells with polysomy and  
516 *ERBB2* amplification (Figure 6 a). Cells in this second category (with or without polysomy) showed  
517 clear SE17 signals with clusters of *ERBB2* signals, which are considered to be a typical signature of  
518 high gene amplification<sup>27,28</sup>. Despite the good quality of the fluorescence images, the clusters for the  
519 *ERBB2* signals were too dense to allow for an accurate quantification of the number of copies, in  
520 order to provide an *ERBB2* amplification score. Concerning the polysomy of chromosome 17, most  
521 amplified cells only presented two copies, but some of the bigger cells presented 3 to 4 copies of the  
522 chromosome. Both cell types can be considered as tumoral cells and although the amount of cancer

523 cells with *ERBB2* amplification was low as compared to blood and mesothelial cells in the sample, the  
524 presence of malignant cells with HER2-positive status in the pleural fluid should provide clinicians  
525 useful prognosis information<sup>29</sup>. Interestingly too, the capacity to distinguish cells with a simple  
526 polysomy from cells with amplification in the same sample gives access to some information about  
527 cellular subpopulation heterogeneity, a question currently considered as extremely important for  
528 better understanding therapeutic escape and improve treatment. Such distinction is not possible with  
529 immunophenotyping.

530 Sample B was also evaluated in a blind process by experienced cytopathologists, using bright field  
531 microscopy after May-Grünwald-Giemsa staining, showing the presence of gigantic cells with tumoral  
532 features (data not shown). This first evaluation was followed by FISH analysis on glass slides, which  
533 detected *ERBB2* amplification in the tumor cells. The quality of the FISH signals obtained by  
534 pathologists was similar to our results on chip and the different cell types immobilized on glass slides  
535 presented the same features as those described above, in particular the presence of *ERBB2* clusters in  
536 HER2-positive cells (Figure 6 b). Thus, the immobilization of cells from a complex sample such as  
537 pleural effusion followed by the HER2 typing with FISH in our COC chip yielded an excellent  
538 agreement with the cytological and molecular analyses performed in the clinics for both samples. It  
539 shows that our approach could be as efficient as the “gold standard”, thus offering a promising  
540 potential for *in situ* analysis of cancer cells. This is the first time that a microfluidic platform for FISH  
541 analysis has been submitted to a blind protocol in the clinics to test its level of maturity. We are now  
542 working in further developments of this system to be able to perform a large scale study.

543



## Conclusion

---

544

545 We have developed a microfluidic platform for Fluorescence In Situ Hybridization, able to provide  
546 quantitative scoring suitable for diagnosis. FISH is the gold standard to assess the presence of gene  
547 amplification (*e.g.* ERBB2), deletion (*e.g.* PTEN) and translocation (*e.g.* EML4-ALK fusion)<sup>30</sup> in tumor  
548 samples, and is used for diagnosis, prognosis and treatment orientation. Based on a new 3D chip  
549 design optimized to allow uniform cell adhesion and a strong reduction of volume as compared to the  
550 conventional methods on glass slides, we developed a new sample treatment and FISH protocol  
551 avoiding the dehydration and drying steps needed on slides. This eliminates several difficulties  
552 associated with drying in closed microchannels, and allows for the full automation of the protocol  
553 under fluidic control. We believe that this change was a major asset to improve the level of  
554 quantitation, reproducibility and accuracy of our approach as compared to previous microfluidic FISH  
555 protocols, and make this approach suitable for clinical diagnosis on real samples and in a routine  
556 setting.

557 This was demonstrated by applying this new method and chip system to the scoring of *ERBB2*  
558 amplification, a major biomarker for breast cancer, associated with the prescription of several new  
559 therapies targeting the HER2 protein. On cell lines, we demonstrated that the method allows not only  
560 mutation detection, as previously achieved in several microfluidic systems<sup>4-7</sup>, but also a quantification  
561 of gene amplification, with a level of reproducibility comparable with that currently achieved on  
562 microslides, considered as the gold standard method. We also demonstrated, in a blind protocol on  
563 two clinical case studies, that our method retains its potential and quality of imaging when dealing  
564 with real clinical samples.

565 Regarding costs, our chip typically uses 10 to 20 times less DNA probes (the most expensive reagent).  
566 The chips themselves are made of COC, a low-cost and medically approved material amenable to  
567 mass microfabrication. Other important contributions to the cost of the assay involve the equipment  
568 needed to perform one experiment, as compared to conventional protocols. In our setup, a simple

569 syringe pump could be used to inject all the reagents sequentially and a calibrated hot plate can be  
570 enough to control the temperature inside the chip, and we believe that automation of the complete  
571 procedure can be easily achieved thus providing a further reduction of the total cost.

572 Last but not least, the reduction of volume consumption of our chips, as compared to current  
573 methods, also concerns the sample. It will thus allow performing more extensive genomic  
574 characterization on small samples. This is particularly timely for two reasons. First, the current  
575 evolution of oncology uncovers an unexpected complexity in the genetic landscape of cancers, and  
576 the number of genes to be screened for diagnosis is regularly increasing. Second, in a trend to  
577 minimize patient's risk and discomfort, diagnosis sampling is evolving towards minimally invasive  
578 methods, such as Fine Needle Aspirates (FNA)<sup>31</sup>, which provide samples in the order of tens to a  
579 hundred microliters. In our validation experiments, we used conservatively 20  $\mu$ L of sample, a volume  
580 typically 10 times smaller than in conventional method, and we could indeed use routinely as little as  
581 5  $\mu$ L without significant degradation of the results. The method thus appears as an ideal companion  
582 for these promising therapeutic developments. More generally, this microfluidic approach opens the  
583 route to an expansion of the use of FISH in various applications including clinical diagnosis, an area in  
584 which it has not reached its full potential due in part to cost and complexity of implementation.

585

## 586 **Acknowledgements**

---

587 The authors thank R. Fert and B. Lemaire (Institut Curie) for their help in microfabrication, B. Coudert  
588 (Institut Curie) for his help with cell culture, L. Sengmanivong (Nikon Imaging Centre, Institut Curie)  
589 for assistance in fluorescence microscopy and O. Delattre (Institut Curie) for useful discussion. This  
590 work was supported by EU funding (FP7 CAMINEMS and DIATOOLS projects) and by Institut Curie (PIC  
591 "residual disease" program).

592

# Bibliography

---

593

- 594 1. C. L. Arteaga, M. X. Sliwkowski, C. K. Osborne, E. A. Perez, F. Puglisi, and L. Gianni, *Nat. Rev.*  
595 *Clin. Oncol.*, 2012, **9**, 16–32.
- 596 2. A. C. Wolff, M. E. H. Hammond, D. G. Hicks, M. Dowsett, L. M. McShane, K. H. Allison, D. C.  
597 Allred, J. M. S. Bartlett, M. Bilous, P. Fitzgibbons, W. Hanna, R. B. Jenkins, P. B. Mangu, S. Paik,  
598 E. A. Perez, M. F. Press, P. A. Spears, G. H. Vance, G. Viale, and D. F. Hayes, *J. Clin. Oncol.*,  
599 2013, **31**, 3997–4013.
- 600 3. O. P. Kallioniemi, A. Kallioniemi, W. Kurisu, A. Thor, L. C. Chen, H. S. Smith, F. M. Waldman, D.  
601 Pinkel, and J. W. Gray, *PNAS*, 1992, **89**, 5321–5.
- 602 4. V. J. Sieben, C. S. Debes-Marun, L. M. Pilarski, and C. J. Backhouse, *Lab Chip*, 2008, **8**, 2151–6.
- 603 5. A. Zanardi, D. Bandiera, F. Bertolini, C. A. Corsini, G. Gregato, P. Milani, E. Barborini, and R.  
604 Carbone, *Biotechniques*, 2010, **49**, 497–504.
- 605 6. I. Vedarethinam, P. Shah, M. Dimaki, Z. Tumer, N. Tommerup, and W. E. Svendsen, *Sensors*,  
606 2010, **10**, 9831–9846.
- 607 7. C.-H. Tai, C.-L. Ho, Y.-L. Chen, W. L. Chen, and G.-B. Lee, *Microfluid. Nanofluidics*, 2013, **15**,  
608 745–752.
- 609 8. Y. Liu, B. Kirkland, J. Shirley, Z. Wang, P. Zhang, J. Stembridge, W. Wong, S. Takebayashi, D. M.  
610 Gilbert, S. Lenhert, and J. Guan, *Lab Chip*, 2013, **13**, 1316–1324.
- 611 9. E. Berthier, E. W. K. Young, and D. Beebe, *Lab Chip*, 2012, **12**, 1224–37.
- 612 10. P. S. Nunes, P. D. Ohlsson, O. Ordeig, and J. P. Kutter, *Microfluid. Nanofluidics*, 2010, **9**, 145–  
613 161.
- 614 11. G. Schelcher, C. Guyon, S. Ognier, S. Cavadias, E. Martinez, V. Taniga, L. Malaquin, P. Tabeling,  
615 and M. Tatoulian, *Lab Chip*, 2014.
- 616 12. A. Bruchet, V. Taniga, S. Descroix, L. Malaquin, F. Goutelard, and C. Mariet, *Talanta*, 2013,  
617 **116**, 488–494.
- 618 13. S. Miserere, G. Mottet, V. Taniga, S. Descroix, J.-L. Viovy, and L. Malaquin, *Lab Chip*, 2012, **12**,  
619 1849–1856.
- 620 14. H. Becker and L. Locascio, *Talanta*, 2002, **56**, 267–287.
- 621 15. H. Becker and C. Gärtner, *Anal. Bioanal. Chem.*, 2008, **390**, 89–111.
- 622 16. G. Mottet, K. Perez-Toralla, E. Tulukcuoglu, F.-C. Bidard, J.-Y. Pierga, I. Draskovic, A. Londono-  
623 Vallejo, S. Descroix, L. Malaquin, and J. Louis Viovy, *Biomicrofluidics*, 2014, **8**, 024109.

- 624 17. K. Perez-Toralla, J. Champ, R. Mohamadi, O. Braun, L. Malaquin, J.-L. Viovy, and S. Descroix,  
625 *Lab Chip*, 2013, **13**, 4409–4418.
- 626 18. I. R. G. Ogilvie, V. J. Sieben, C. F. A. Floquet, R. Zmijan, M. C. Mowlem, and H. Morgan, *J.*  
627 *Micromechanics Microengineering*, 2010, **20**, 065016.
- 628 19. J. Zhang, C. Das, and Z. H. Fan, *Microfluid. Nanofluidics*, 2008, **5**, 327–335.
- 629 20. D. Mazia, G. Schatten, and W. Sale, *J. Cell Biol.*, 1975, **66**, 198.
- 630 21. Q. Zhang, L. Zhu, H. Feng, S. Ang, F. S. Chau, and W.-T. Liu, *Anal. Chim. Acta*, 2006, **556**, 171–7.
- 631 22. J. Sibarita, *Adv. Biochem. Eng. Biotechnol.*, 2005, **95**, 201–243.
- 632 23. V. J. Sieben, C. S. Debes Marun, P. M. Pilarski, G. V Kaigala, L. M. Pilarski, and C. J. Backhouse,  
633 *IET nanobiotechnology*, 2007, **1**, 27–35.
- 634 24. J. Szöllösi, M. Balázs, B. G. Feuerstein, C. C. Benz, and F. M. Waldman, *Cancer Res.*, 1995, **2**,  
635 5400–5407.
- 636 25. P. Paterlini-Brechot and N. L. Benali, *Cancer Lett.*, 2007, **253**, 180–204.
- 637 26. P. Bunn, B. Helfrich, and A. Soriano, *Clin. cancer*, 2001, **7**, 3239–3250.
- 638 27. J. Klijanienko, J. Couturier, M. Galut, A. K. El-Naggar, Z. Maciorowski, E. Padoy, V. Mosseri, and  
639 P. Vielh, *Cancer*, 1999, **87**, 312–318.
- 640 28. J. Couturier, A. Vincent-Salomon, M.-C. Mathieu, A. Valent, and A. Bernheim, *Pathol. Biol.*,  
641 2008, **56**, 375–9.
- 642 29. K. Kunitomo, S. Inoue, F. Ichihara, K. Kono, H. Fujii, Y. Matsumoto, and A. Ooi, *Hum. Pathol.*,  
643 2004, **35**, 379–381.
- 644 30. E. Pailler, J. Adam, A. Barthemy, M. Oulhen, N. Auger, A. Valent, I. Borget, D. Planchard, M.  
645 Taylor, F. André, J. C. Soria, P. Vielh, B. Besse, and F. Farace, *J. Clin. Oncol.*, 2013, **31**, 2273–  
646 2282.
- 647 31. C. Bozzetti, R. Nizzoli, A. Guazzi, M. Flora, C. Bassano, P. Crafa, N. Naldi, and S. Cascinu, *Ann.*  
648 *Oncol.*, 2002, **13**, 1398–1403.

649

650

651

652

653

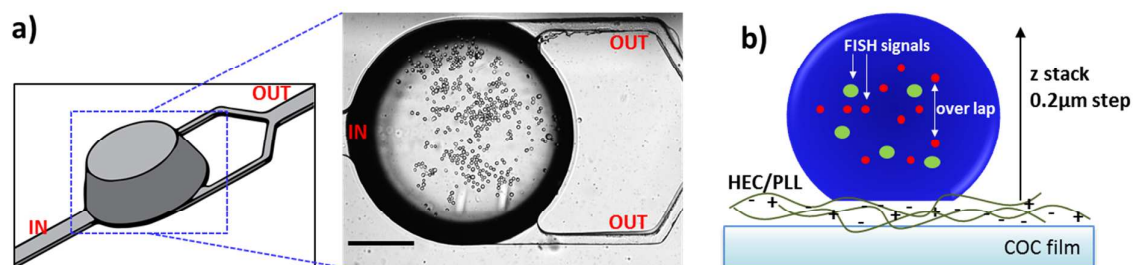
654

655 **Figures:**

---

656

657



658

659

660

661

662

663

Figure 1 : a) Schematic view of the COC chip showing the "3D" chamber (height=0.38 mm, bottom diameter=1 mm) and the narrow microchannels (height=30 μm, width=60 μm) (left) and a micrograph showing the cells immobilized at the bottom of the chamber (right) at low magnification using bright field microscopy (scale bar=300 μm), b) Schematic representation of cells immobilized on the treated surface of the COC chip for FISH analysis.

664

665

Step on the FISH protocol	Glass slide		COC chip		
	Volumes ( $\mu\text{L}$ )	Incubation Time (min/ $T^\circ$ )	Volumes ( $\mu\text{L}$ )	Incubation Time (min/ $T^\circ$ )	Pressure (kPa)
1 Cell adhesion	200 ( $\sim 2 \times 10^5$ cells)	O.N. <sup>a</sup> /37°C	20 ( $\sim 2 \times 10^4$ cells)	30/R.T. <sup>b</sup>	1-4
2 1st washing	25, 000	2 /37 °C	200	-	10- 20
3 Enzymatic digestion	25, 000 [C]=0.05 $\mu\text{g}/\text{mL}$	7 /37 °C	100 [C]=1 $\mu\text{g}/\text{mL}$	7/37°C	10-20
4 2nd washing	(2 x) 25, 000	4 /37 °C	150	-	10-20
5 Fixation	25, 000	20 /5°C	100	20 /5°C	10-20
6 3rd washing	25, 000 25, 000	10/37°C 2/R.T.	(2 x) 200	10/37°C	35
7 Dehydration and drying	(3 x) 25, 000	(3 x) 2/R.T. 15/R.T.	<b>NO</b>	<b>NO</b>	<b>NO</b>
8 Probe injection and denaturation	10 [C]=1X	15/75°C	5 [C]=0.5 X	15/75°C	35
9 Hybridization		O.N. /37°C		O.N. /37°C	
10 Post-hybridization washing 1	(2 x) 25, 000	2/72°C	(2 x) 100	4/72°C	30-35
11 Post-hybridization washing 2	(2 x) 25, 000	2/72°C	(2 x) 100	-	30-35
12 Dehydration and drying	(3 x) 25, 000	3 x 2/R.T. 15/R.T.	<b>NO</b>	<b>NO</b>	<b>NO</b>
13 Counter staining	10	10/R.T.	5	10/R.T.	35

666

667 **Table 1 : Steps of the FISH protocol on standard glass slide vs. COC chip, showing the reduction of volumes of**  
668 **reagents and changes in concentration of pepsin and probe solutions. No dehydration and drying steps are**  
669 **performed in the protocol on chip.**

670

a:O.N.=Over night, b: R.T.= Room temperature

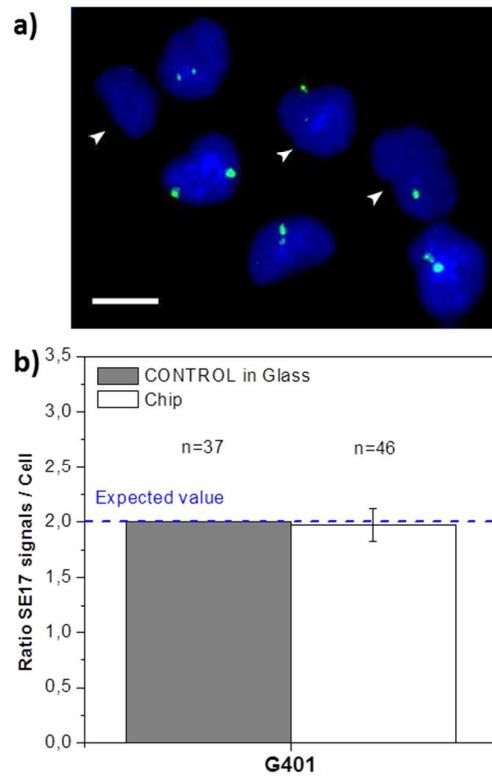
671

672

673

674

675



676

677

678

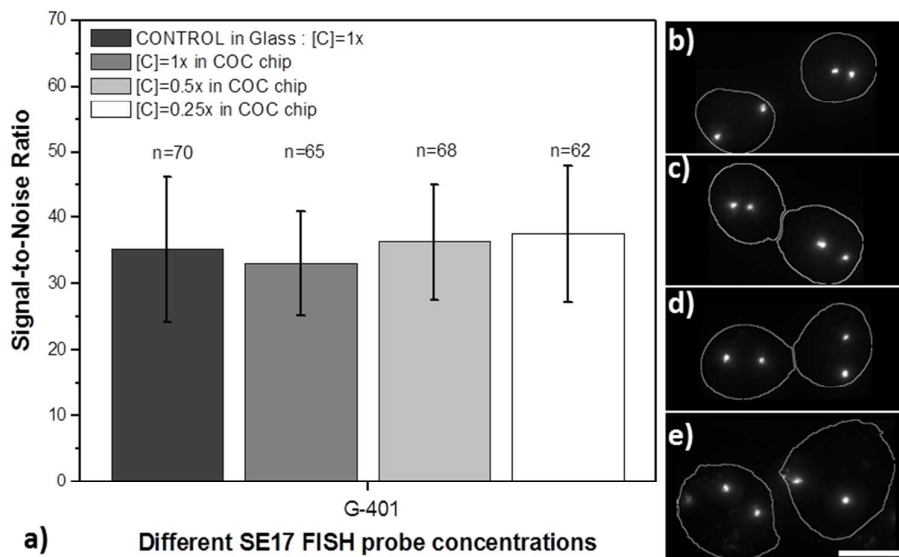
679

680

681

**Figure 2 : G-401 cell lines after FISH with the SE17 centromeric probes. a) Fluorescence imaging of FISH results before optimization of the miniaturized protocol on COC chip. Several nuclei (white arrows) only present one or no signal for the SE17 centromeric probe, as a consequence of incomplete EtOH drying (scale bar=5  $\mu$ m). b) Performance of the flow-through FISH protocol on chip after optimization, compared to the standard protocol on glass slide. Error bars show the Standard Deviation (S.D.)**

682



683

684

685

686

687

688

689

Figure 3 : a) Signal-to-Noise ratio measured on G-401 cell lines after FISH analysis of the signals from the SE17 centromeric probes on glass slides with the standard probe concentration (e: [C]=1x) and on chip with different probe concentrations (b:[C]=1x, c:[C]=0.5x, d:[C]=0.25x, scale bar=5 μm). SNR was measured as the ratio of the corrected maximum intensity of the peaks from FISH signals and the standard deviation of the intensity background coming from the cell nuclei. All measured cells contained 2 distinct SE17 signals. Error bars show the S.D.

690

691

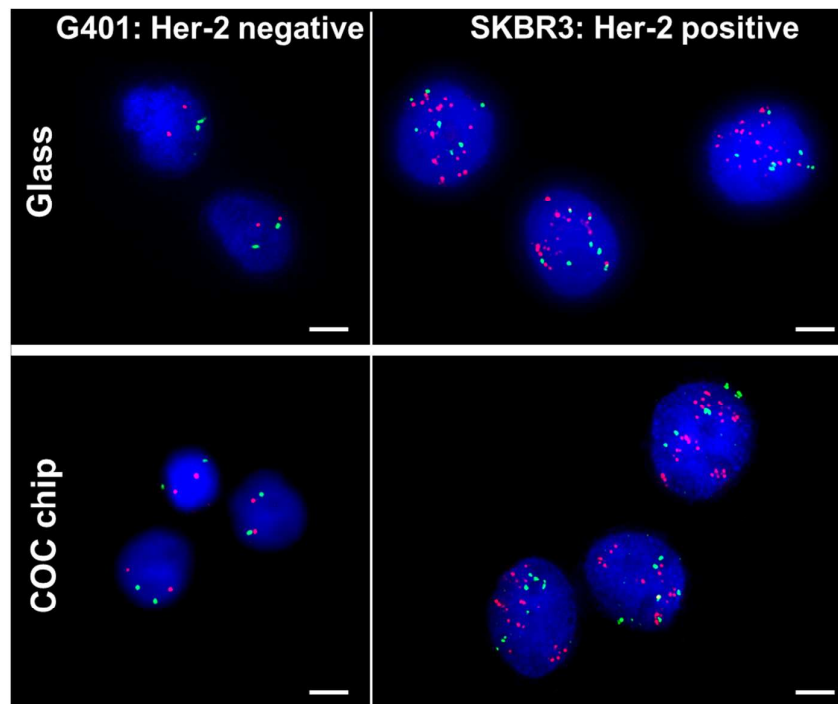
692

693

694

695





696

697

698

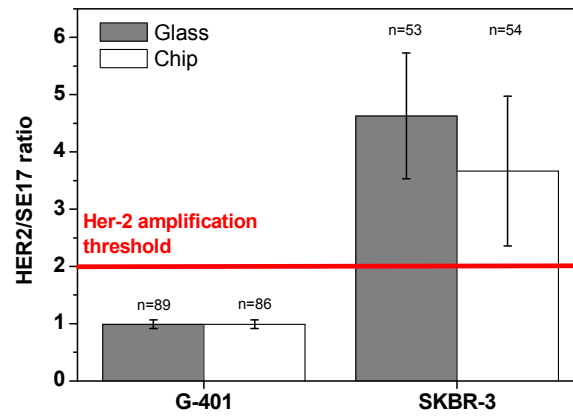
Figure 4 : High magnification fluorescence imaging of FISH results on glass slide (a, b) and on COC chip(c, d) for the HER2 typing of G-401(a, c) and SKBR-3 (b, d) cell lines (scale bar=2  $\mu\text{m}$ )

699

700

701

702



703

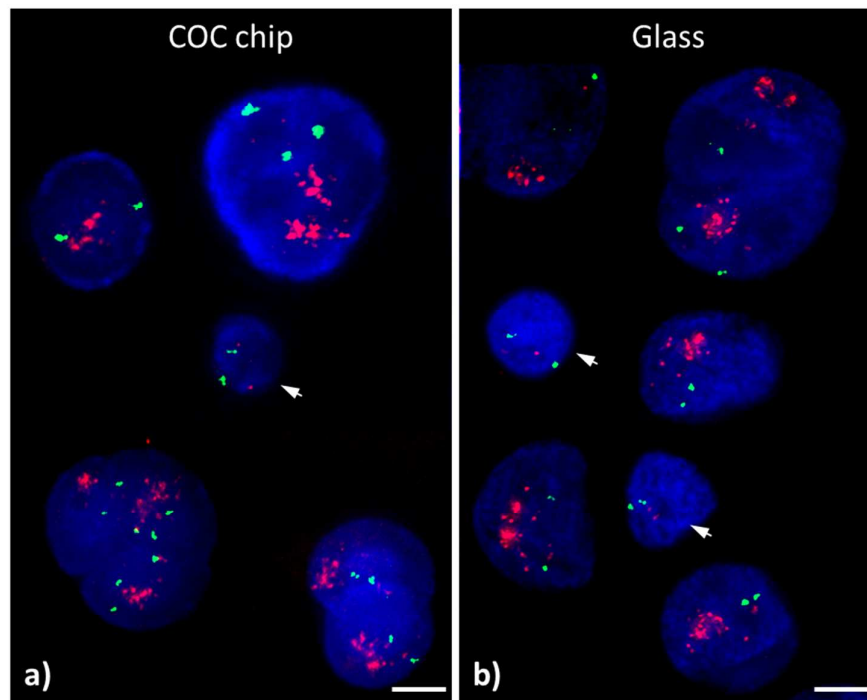
704

705

Figure 5 : FISH protocol validation on chip vs glass slides using two control cell lines with different karyotype and different HER2 status. Error bars show the S.D.

706

707



708

709

710

Figure 6 : FISH results for HER2 typing of cells from a pleural effusion from a breast cancer patient (Sample B) on COC chip (a) and on glass slide (b). White arrow shows possible leucocytes (scale bar=5  $\mu$ m)

711

712